Volume 23
Number 24
28 June 2021
Pages 4239–4410

CrystEngComm

rsc.li/crystengcomm

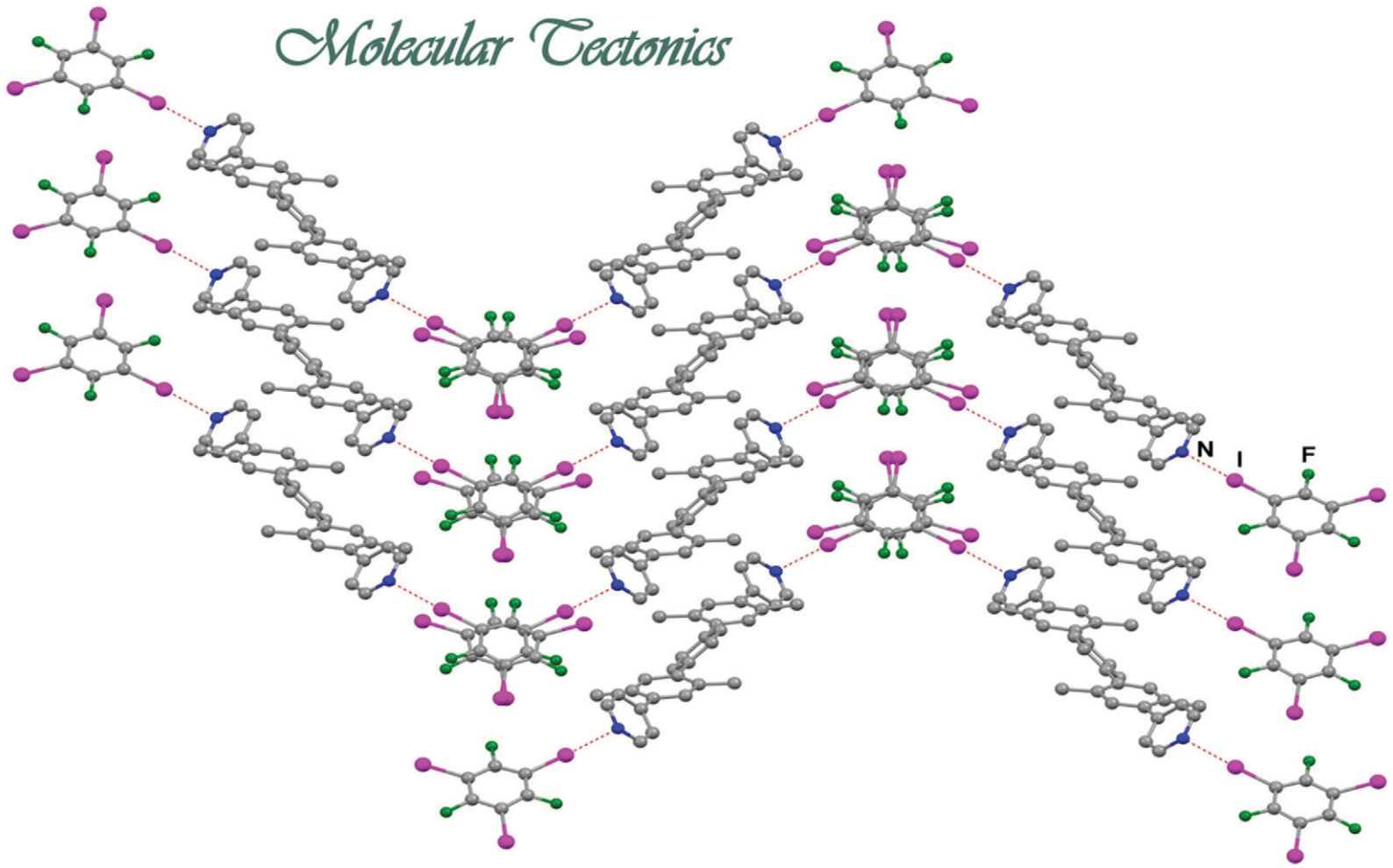

ISSN 1466-8033

ROYAL SOCIETY OF CHEMISTRY

PAPER

Véronique Bulach, Mir Wais Hosseini, Stefan Bräse *et al.*
Halogen-bonded one-dimensional chains of functionalized ditopic bipyridines co-crystallized with mono-, di-, and triiodofluorobenzenes

CrystEngComm

ROYAL SOCIETY OF CHEMISTRY

PAPER

View Article Online
View Journal | View Issue

Cite this: *CrystEngComm*, 2021, **23**, 4247

Halogen-bonded one-dimensional chains of functionalized ditopic bipyridines co-crystallized with mono-, di-, and triiodofluorobenzenes†

Elena Vulpe,[a] Sylvain Grosjean,[b] Zahid Hassan,[c] Véronique Bulach,*[a] Mir Wais Hosseini*[a] and Stefan Bräse*[bcd]

Received 14th April 2021,
Accepted 12th May 2021

DOI: 10.1039/d1ce00494h

rsc.li/crystengcomm

A series of halogen-bonded (XB) discrete, one-dimensional (1D) linear and zigzag supramolecular architectures by co-crystalizing a sterically hindered class of homologous ditopic *para*-xylenes bearing bipyridyl moieties at peripheries with mono-, di-, and triiodofluorobenzene as XB donor components were prepared. The solid-state structures investigated by X-ray diffraction on single crystals show that the molecular geometry of the tectons and halogen bond directionality translates into corresponding XB co-crystals and display a conformational twist at the planes of *para*-xylene with the adjacent aromatic rings. The bipyridine tectons grafted with photo-responsive azobenzene (–N=N–) side-group, once integrated into the halogen-bonded chains, can be remotely modulated by light, thus being applicable for controlling structure and innovative applications possibilities.

Self-assembly of small molecules/tectons into hierarchically-organized supramolecular assemblies and structuring materials by a dimensional organizing principle, such as molecular arrangements "along the chain" in polymers,[1] and controlled arrangements in the second and third dimensions "in space" to obtain periodic assemblies, has been the subject of extensive recent research.[2] Self-assembly of molecular tectons through non-covalent strategies, for instance, metal coordination-driven approaches, and supramolecular interactions of π–π stacking, halogen-bonding or better-known hydrogen bonds form diverse hierarchically-organized (ranging from 1D to 3D molecular arrangements) supramolecular assemblies.[3]

Tuning the structure and functions of supramolecular architecture at the molecular level *via* tecton design (size, shape, geometry, and directionality) and controlling forces that hold tectons together is of utmost relevance. Halogen-bonded co-crystal engineering, *i.e.* using non-covalent interactions involving halogens as electrophile species,[4] has been an effective and reliable tool to control and direct supramolecular assembly processes and give rise to versatile chemicophysical properties.[5] For instance, recent examples of emerging supramolecular materials include electrical conductivities and field-effect transistors,[6] organic photonics,[7] and a diverse area of liquid crystals, anion recognition, and other function-inspired materials.[8] In this contribution, we report the formation of a series of halogen-bonded supramolecular architectures involving a sterically hindered class of homologous ditopic *para*-xylene bearing bipyridyl moieties at peripheries co-crystallized with mono-, di-, and triiodofluorobenzenes as XB donors (Fig. 1).

Bipyridyl-based molecular tectons, the most widely used nitrogen-containing aromatic heterocyclic scaffolds, generate

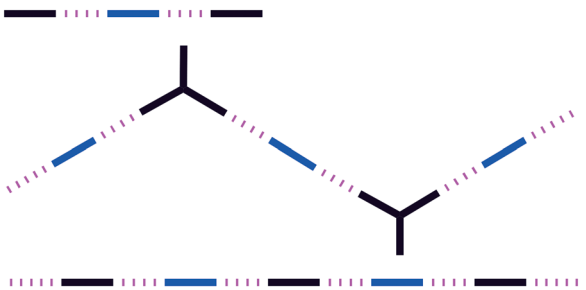

Fig. 1 Depiction of the bipyridine molecular tectons (blue) and halogen bond donors directionality (black) that dictate the corresponding halogen bonds (dotted lines) to form discrete (top), zigzag (middle) and 1D linear (bottom) supramolecular architectures.

[a] *Molecular Tectonics Laboratory, UMR UDS-CNRS, 7140 & icFRC, University of Strasbourg, F-67000, Strasbourg, France. E-mail: hosseini@unistra.fr*
[b] *Soft Matter Synthesis Laboratory, Institute for Biological Interfaces 3 (IBG 3), Karlsruhe Institute of Technology (KIT), Hermann-von-Helmholtz-Platz 1, 76344 Eggenstein-Leopoldshafen, Germany*
[c] *Institute of Organic Chemistry (IOC), Karlsruhe Institute of Technology (KIT), Fritz Haber-Weg 6, 76131, Karlsruhe, Germany. E-mail: braese@kit.edu*
[d] *Institute of Biological and Chemical Systems, Functional Molecular Systems (IBCS FMS), Karlsruhe Institute of Technology (KIT), Hermann-von-Helmholtz-Platz 1, 76344 Eggenstein-Leopoldshafen, Germany*

† Electronic supplementary information (ESI) available: Materials and methods, analytical and crystallographic data. CCDC 2076758–2076764. For ESI and crystallographic data in CIF or other electronic format see DOI: 10.1039/d1ce00494h

highly ordered diverse supramolecular assemblies.[9] Incorporating ambitious functional features into such molecular tectons, for instance, stereochemistry, switchability, photo-tunability or responsiveness that operates under specific physical or chemical environments (*e.g.*, light or mechanical forces *etc.*), thus being applicable for dynamic photo-, and mechanochemical control is of fundamental relevance because these molecular features could be inherited once assembled into made-to-order materials.[10] Model ditopic pyridine-bearing molecular tectons with different sizes/length (by including benzene rings as spacer groups) and grafted with photo-responsive azobenzene (–N═N–) moiety (Scheme 1) were synthesized following a modular synthesis approach by stepwise Mills and Suzuki–Miyaura cross-coupling reaction (see the ESI† S.1.2). As the solubility of the linear oligoarenes drops when their length increases, methyl or longer alkyl groups are often introduced to increase the solubility of the polyaromatic systems.[11] On the other hand, sterically hindered components (*para*-xylenes) cause variations in electronic and conformational properties due to the consequential twist between adjacent aromatic units' planes.

We have recently incorporated chiral bipyridines to construct homochiral 1D and 2D crystalline coordination networks.[12] The dimensionality of the latter and their packing in the crystal depends on the nature of the tectons, chiral side functionalities grafted with tectons, and crystallization solvent system. The particular role of the halogen bond directionality using *ortho*-, *meta*- and *para*-isomers of diiodotetrafluorobenzene that dictates the co-crystals architecture has also been demonstrated.[13] During this investigations, we studied halogen bonding interactions of a sterically hindered class of modular bipyridines **I**, **II** and **III** in combination with the monoiodoperfluorobenzene (**IFB**), diiodotetrafluorobenzene (**DIFB**), and triiodotrifluorobenzene (**TIFB**) as XB donor components respectively, focusing on the particular role of the halogen bond directionality and denticity.

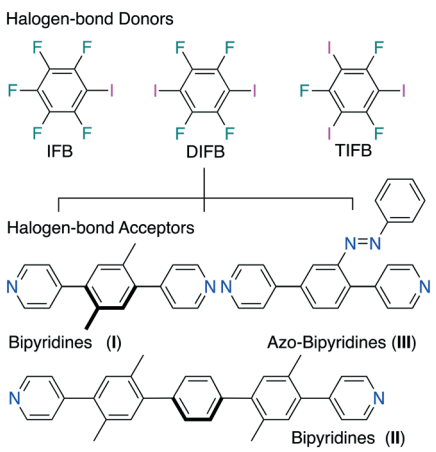

Scheme 1 Bipyridine tectons (I–III) co-crystallized with **IFB**, **DIFB**, and **TIFB** as halogen-bond donors in supramolecular systems.

Initially, (**IFB**) was introduced as a stopper in the presence of the bipyridyl tectons (**I–III**) to synthesize halogen-bonded discrete co-crystals that could serve as primary references in our studies for comparing the influence of the N···I interactions on the overall bond angles and distances. Several crystallization conditions with different ratios (**I–III**) *vs.* **IFB** were analyzed. The same holds for **TIFB** (see the ESI† S.1.3). In the case of **DIFB**, equimolar stoichiometry was used. When a 1 : 2 tecton/**TIFB** ratio was used, well-defined halogen-bonded co-crystals were grown for both **I** and **II**. The 3 : 2 ratio of **I**/**TIFB** leads to forming a network, while compound **II** crystallizes alone without any halogen-bonded co-assembly. Bipyridyl tecton **III** resulted into amorphous powder.

To obtain a crystal structure for solid-state diffraction, **I** and **II** and **IFB** were dissolved in ethanol (1 mL), and after two days, light yellow well-defined crystals were obtained (Fig. 2). The single-crystal X-ray diffraction analysis revealed, in both cases, the formation of discrete halogen-bonded co-crystals. For the two supramolecular entities, the N···I bonds was measured 3.53 Å, 19–20% shorter than the sum of van der Waals radii. The connectivity is the same in both structures; however, the crystal packing shows tecton-dependent differences. For the shorter tecton **I**, a herringbone arrangement with **IFB** molecules between the layers was observed (Fig. 2a), while for the longer bipyridine tecton, including terphenyl moiety as a spacer, linear chains packed in a parallel fashion were formed (Fig. 2b). Interestingly, for the herringbone structure, no π–π interactions were observed, C–F···H–C contacts with C···F distances close to 3.5 Å are identified. Within the tecton **I**, the Npy–Npy distance is equal to 11.4 Å, and the tilt angle between the pyridine mean plane and the xylene moiety is about 47°, a feature subject to significant changes depending on the coordinating iodine-based tectons. The tilt angle between the pyridine and the **IFB** is shown at 23°.

For the bipyridyl tecton **II**, the Npy–Npy distance is equal to 20.1 Å, and the dihedral angle between pyridine moiety mean planes and xylene moiety is about 40° while the tilt angle between the xylene moieties and the benzene ring is 44°. The tilt angle between the pyridine and the **IFB** is 18°. As for tecton **I**, no π–π or C–F···H–C interactions were observed.

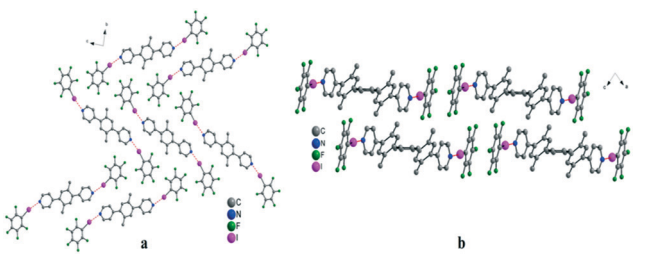

Fig. 2 View of packing of XB co-crystals formed between **IFB** and molecular bipyridyl tecton **I** (a; left side) and tecton **II** (b; right side). Hydrogen atoms are omitted for clarity.

By combining bipyridyl core **I** or **II** with **DIFB**, the formation of two infinite linear chains of the same topology was observed (Fig. 3). Both structures present the same N···I distance of 2.78 Å with stabilizing C–F···H–C contacts (C···F of *ca.* 3.4 Å) connecting neighbouring layers.

The structural differences become apparent when looking at the angles between the pyridine mean plane and the **DIFB** moiety; for the shorter tecton, the angle is *ca.* 77°, while for the longer tecton **II**, the angle is 32°. Within the bipyridyl tecton **I**, as emphasized before, there is also a shift of about 19° for the angle between the mean plane of the pyridine (Pymp) and the mean plane of the xylene (Xymp) moiety. For the bipyridyl tecton **II**, the change is in the 5–7° range (see ESI† Table S1).

By combining tecton **I** or **II** with **TIFB**, the formation of only two halogen bonds was observed, indicating that only two out of the three iodines take part in the formation of the XB assembly. There are limitations observed to the formation of halogen bonds with a single aromatic halogen donor. To gain insight on the contributing factors controlling the formation of multiple halogen bonds, co-crystallization of the symmetrical 1,3,5-triiodo-2,4,6-trifluorobenzene (**TIFB**) with different bipyridyl donors has been previously investigated and identified co-crystals formation with only two N···I halogen bonds instead of anticipated three N···I halogen bonds.[14] Packing constraints were presumed to dominate over the possibility of the formation of a third N···I intermolecular halogen-bonding interaction. By positioning **TIFB** and I^- ions as a judicious choice of the XB-acceptor to overcome both the electronic and the steric aspects, mutual induced coordination in halogen-bonded anionic assemblies with (6,3) cation-templated topologies have been identified.[15] Using a 3 : 2 tecton/**TIFB** ratio, in the case of **II**, crystals were only composed of the bipyridyl tecton. However, in the case of the tecton **I**, the formation of a zigzag chain was observed. The co-crystal displays two distinct N···I bonds of 2.85 and 2.91 Å, with two different angles between the mean plane of the pyridyl moiety and the **TIFB** plane of *ca.* 43° and 47°. The overall packing shows π–π stacking interactions between **TIFB** moieties with a distance of *ca.* 3.5 Å (Fig. 4a).

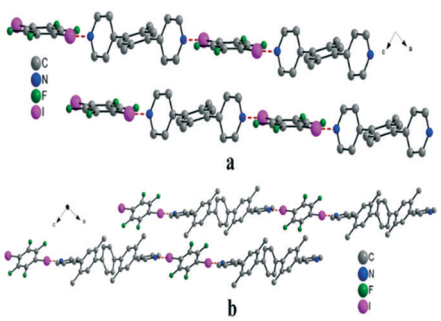

Fig. 3 View of 1D linear chains formed between **DIFB** and bipyridyl tecton **I** (a; top) and tecton **II** (b; bottom). Hydrogen atoms are omitted for clarity.

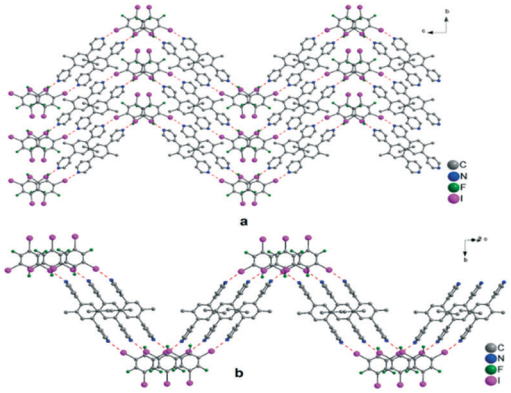

Fig. 4 View of the zigzag chains formed through two N···I halogen bonds between **I** and **TIFB** (3 : 2 ratio) (a; top); a portion of the chains formed through two N···I halogen bonds between **I** and **TIFB** (1 : 2 ratio) (b; bottom). Hydrogen atoms are omitted for clarity.

A 1 : 1 chloroform/ethanol mixture of **I** or **II** with **TIFB** afforded two different types of networks. In the case of **I**, a network with a 1 : 2 ratio of tectons was formed. Whereas for **II**, a network with a 2 : 1 ratio was generated. For the 1D network based on tecton **I**, the formation of two N···I halogen bonds was observed (Fig. 4b). The infinite chain obtained using a 1 : 2 stoichiometry is different from the one obtained using a 3 : 2 stoichiometry. Within the halogen bond acceptor tecton, a change in the angle of *ca.* 19° between the mean plane of the pyridyl and the *para*-xylene molecule was observed. This may be attributed to a less restrained overall π-system compared to tecton **II**, for which the difference in angles is much less pronounced. No interactions between chains could be detected in this case. For the co-crystals based on tecton **II**, only one N···I halogen bond per **TIFB** molecule was observed. For this 2 : 1 adduct, the chains are arranged in a herringbone fashion. The **TIFB** within consecutive layers is stacked in an offset manner (Fig. 5). In contrast with the structure mentioned above obtained with the tecton **I**, two F···I (3.11 Å) intermolecular contacts (distance shorter by 10% to the sum of van der Waals radii) were formed. In this

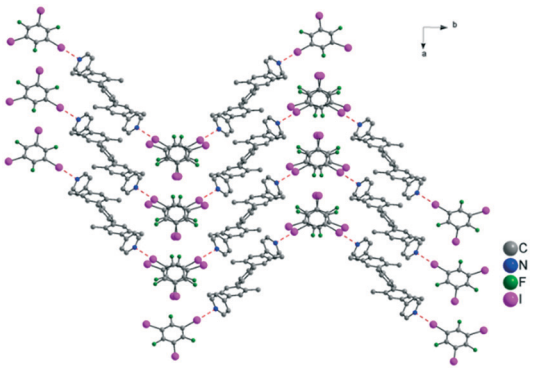

Fig. 5 A portion of the structure obtained by combining the tecton **II** and **TIFB** through one N···I halogen bonds. Hydrogen atoms are omitted for clarity.

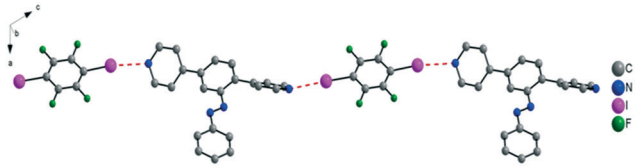

Fig. 6 View of the linear chains formed through two N···I halogen bonds between III and TIFB. Hydrogen atoms are omitted for clarity.

case, the C–F···I angles are almost identical and close to *ca.* 163°, which suggests a type **I** halogen–halogen interactions.

The ditopic bipyridine tecton **III**, grafted with photo-responsive azobenzene (–N═N– moiety), is of particular interest. We have previously demonstrated the design and fabrication of diverse azobenzene-containing photo-tunable nanosystems, such as nanoporous crystalline thin-films with controlled diffusion properties,[16] and surface-mounted hybrid systems.[17] These 'smart' material applications are based on the well-designed azobenzene-containing tectons with characteristic photoswitchable features, imparting desired tunable functions once assembled into materials. Similarly, bipyridine tecton **III** bearing a –N═N– azobenzene photo-responsive moiety, once integrated into halogen-bonded chains, can be remotely modulated by light, thus being applicable for controlling structure and innovative applications possibilities.

A similar procedure, the co-crystalization of tecton **III** and **DIFB**, resulted in a linear chain, resulting from two N···I bonds with 2.85 Å and 2.88 Å distances with angles between C–I···N around 170°. Within the network, the *E* isomer (or *trans*-) of azobenzene was observed (Fig. 6). The angles between the mean plane of the **DIFB** and the connecting pyridine moiety are 41° and 42°. Within the tecton, the angle between the two pyridyl moieties is 82°, and the dihedral angle between the pyridyl units and the central benzene moiety is 39°. The **DIFB** moieties belonging to the same plane are π–π stacked (centroid distance of 3.6 Å) with a benzene moiety of the azobenzene group of consecutive layers. The fluorine atoms of the **DIFB** also formed intermolecular H···F bonds with pyridyl units (dC—F in the 3.12–3.5 Å range), as well as between **DIFB** moiety and the protons of the benzene moiety from the azobenzene function (C···F = 3.27 Å).

The chains formed through two N···I halogen bonds showed that the –N═N– group within the co-crystals is not involved in further molecular interactions that could be further exploited in photoisomerization to explore switchable properties of the systems. Research efforts towards the development of photo-tunable halogen-bonded 'smart' supramolecular systems are currently underway in our laboratories.

Conclusions

In this study, we presented the formation of a series of halogen-bonded assemblies, including discrete co-crystals, 1D linear chains, and zigzag supramolecular architectures by co-crystallizing a sterically hindered class of homologous ditopic *para*-xylenes bearing bipyridyl moieties at peripheries with mono-, di-, and triiodofluorobenzene components as XB donors. The halogen bond directionality and denticity of the iodofluorobenzene dictate co-crystals architecture has been demonstrated. The solid-state structures investigated by X-ray diffraction on single crystals have shown that the molecular geometry of the small molecular tectons and halogen bond directionality ultimately translates into the corresponding XB 1D linear and zigzag chains and displays a conformational twist between the planes of the *para*-xylenes with the adjacent aromatic rings.

Conflicts of interest

The authors declare no competing financial interest for this article.

Acknowledgements

ChiraNET – Synthesis of Chiral Porous Crystals for Racemic Resolution – an interregional research cooperation project between the KIT, the Université de Strasbourg and the Universität Kaiserslautern is greatly acknowledged for financial contributions. The University of Strasbourg, CNRS, Institut Universitaire de France (IUF), and the International Center for Frontier Research in Chemistry (icFRC) are acknowledged for financial support to the Strasbourg group. The authors acknowledge support provided by Deutsche Forschungsgemeinschaft (DFG) under Germany's Excellence Strategy – 3DMM2O – EXC-2082/1-390761711.

Notes and references

1 J. F. Lutz, J. M. Lehn, E. W. Meijer and K. Matyjaszewski, *Nat. Rev. Mater.*, 2016, **1**, 1–14.
2 O. M. Yaghi, M. J. Kalmutzki and C. S. Diercks, *Introduction to Reticular Chemistry: Metal–Organic Frameworks and Covalent Organic Frameworks*, Wiley-VCH, Weinheim, Germany, 2019.
3 D. B. Amabilino and P. A. Gale, *Chem. Soc. Rev.*, 2017, **46**, 2376–2377.
4 (*a*) G. R. Desiraju, P. S. Ho, L. Kloo, A. C. Legon, R. Marquardt, P. Metrangolo, P. Politzer, G. Resnati and K. Rissanen, *Pure Appl. Chem.*, 2013, **85**, 1711–1713; (*b*) C. B. Aakeroy, M. Fasulo, N. Schutheiss, J. Desper and C. Moore, *J. Am. Chem. Soc.*, 2007, **129**, 13772–13773; (*c*) L. Brammer, E. A. Bruton and P. Sherwood, *Cryst. Growth Des.*, 2001, **1**, 277–290; (*d*) A. Mukherjee, S. Tothadi and G. R. Desiraju, *Acc. Chem. Res.*, 2014, **47**, 2514–2524; (*e*) K. Rissanen, *CrystEngComm*, 2008, **10**, 1107–1113.
5 (*a*) G. Cavallo, P. Metrangolo, R. Milani, T. Pilati, A. Priimagi, G. Resnati and G. Terraneo, *Chem. Rev.*, 2016, **116**, 2478–2601; (*b*) A. Priimagi, G. Cavallo, P. Metrangolo and G. Resnati, *Acc. Chem. Res.*, 2013, **46**, 2686–2695; (*c*) L. C. Gilday, S. W. Robinson, T. A. Barendt, M. J. Langton, B. R. Mullaney and P. D. Beer, *Chem. Rev.*, 2015, **115**, 7118–7195;

(*d*) W. T. Pennington, G. Resnati and M. S. Taylor, *CrystEngComm*, 2013, **15**, 3057–3057.

6 L. Sun, Y. Wang, F. Yang, X. Zhang and W. Hu, *Adv. Mater.*, 2019, **31**, 1902328.

7 (*a*) Y. Liu, A. Li, S. Xu, W. Xu, Y. Liu, W. Tian and B. Xu, *Angew. Chem., Int. Ed.*, 2020, **59**, 15098–15103; (*b*) M. P. Zhuo, Y. C. Tao, X. D. Wang, Y. Wu, S. Chen, L. S. Liao and L. Jiang, *Angew. Chem., Int. Ed.*, 2018, **57**, 11300–11304; (*c*) L. Bai, P. Bose, Q. Gao, Y. Li, R. Ganguly and Y. Zhao, *J. Am. Chem. Soc.*, 2017, **139**, 436–441; (*d*) Q. N. Zheng, X. H. Liu, T. Chen, H. J. Yan, T. Cook, D. Wang, P. J. Stang and L. J. Wan, *J. Am. Chem. Soc.*, 2015, **137**, 6128–6131; (*e*) M. Boterashvili, M. Lahav, S. Shankar, A. Facchetti and M. E. van der Boom, *J. Am. Chem. Soc.*, 2014, **136**, 11926–11929.

8 (*a*) Y. Huang, Z. Wang, Z. Chen and Q. Zhang, *Angew. Chem., Int. Ed.*, 2019, **58**, 9696–9711; (*b*) X. H. Ding, Y. Z. Chang, C. J. Ou, J. Y. Lin and L. H. Xie, *Natl. Sci. Rev.*, 2020, **7**, 1908–1932; (*c*) G. Berger, J. Soubhyea and F. Meyer, *Polym. Chem.*, 2015, **6**, 3559–3580.

9 (*a*) M. W. Hosseini, *Acc. Chem. Res.*, 2005, **38**, 313–323; (*b*) M. W. Hosseini, *CrystEngComm*, 2004, **6**, 318–322; (*c*) M. W. Hosseini, *Chem. Commun.*, 2005, 5825–5829; (*d*) A. Gorczyński, J. M. Harrowfield, V. Patroniak and A. R. Stefankiewicz, *Chem. Rev.*, 2016, **116**, 14620–14674.

10 Z. Hassan, Y. Matt, S. Begum, M. Tsotsalas and S. Bräse, *Adv. Funct. Mater.*, 2020, 1907625.

11 (*a*) S. Grosjean, Z. Hassan, C. Wöll and S. Bräse, *Eur. J. Org. Chem.*, 2019, 1446–1460; (*b*) S. Grosjean, P. Hodapp, Z. Hassan, C. Wöll, M. Nieger and S. Bräse, *ChemistryOpen*, 2019, **8**, 743–759; (*c*) S. Grunder and J. F. Stoddart, *Chem. Commun.*, 2012, 3158–3160; (*d*) J. C. Barnes, M. Juricek, N. A. Vermeulen, E. J. Dale and J. F. Stoddart, *J. Org. Chem.*, 2013, **78**, 11962–11969.

12 (*a*) P. Larpent, A. Jouaiti, N. Kyritsakas and M. W. Hosseini, *CrystEngComm*, 2019, **21**, 2534–2540; (*b*) P. Larpent, A. Jouaiti, N. Kyritsakas and M. W. Hosseini, *Chem. Commun.*, 2013, 4468–4470.

13 (*a*) M. Saccone, G. Cavallo, P. Metrangolo, A. Pace, I. Pibiri, T. Pilati, G. Resnati and G. Terraneo, *CrystEngComm*, 2013, **15**, 3102–3105; (*b*) A. D. Santis, A. Forni, R. Liantonio, P. Metrangolo, T. Pilati and G. Resnati, *Chem. – Eur. J.*, 2003, **9**, 3974–3983; (*c*) T. Caronna, R. Liantonio, T. A. Logothetis, P. Metrangolo, T. Pilati and G. Resnati, *J. Am. Chem. Soc.*, 2004, **126**, 4500–4501; (*d*) C. C. Robertson, J. S. Wright, E. J. Carrington, R. N. Perutz, C. A. Hunter and L. Brammer, *Chem. Sci.*, 2017, **8**, 5392–5398; (*e*) P. Liu, Z. Li, B. Shi, J. Liu, H. Zhu and F. Huang, *Chem. – Eur. J.*, 2018, **24**, 4264–4267.

14 A. C. B. Lucassen, A. Karton, G. Leitus, L. J. W. Shimon, J. M. L. Martin and M. E. van der Boom, *Cryst. Growth Des.*, 2007, **7**, 386–392.

15 P. Metrangolo, F. Meyer, T. Pilati, G. Resnati and G. Terraneo, *Chem. Commun.*, 2008, 1635–1637.

16 X. Yu, Z. Wang, M. Buchholtz, N. Füllgrabe, S. Grosjean, F. Bebensee, S. Bräse, C. Wöll and L. Heinke, *Phys. Chem. Chem. Phys.*, 2015, **17**, 22721–22725.

17 Z. Wang, A. Knebel, S. Grosjean, D. Wagner, S. Bräse, C. Wöll, J. Caro and L. Heinke, *Nat. Commun.*, 2016, **7**, 13872.